

# Environmental sustainability of fly ash and recycled crushed glass blends: an alternative to natural clay for masonry bricks production

Aneke Frank Ikechukwu <sup>1\*</sup>, Kennedy C. Onyelowe <sup>2</sup>

<sup>1</sup> *Geotechnical and Materials Development Research Group (GMDRg) Civil Engineering Department, University of KwaZulu-Natal, Durban 4004, South Africa*

<sup>2</sup> *Senior Lecturer, Department of Civil and Mechanical Engineering, Kampala International University, Kampala, Uganda*

## ABSTRACT

Waste utilization as an alternative for masonry bricks has proven to compensate for the dwindling natural construction materials particularly clay. Currently, South African municipalities are struggling to update their effective waste management techniques. Improper waste management is one of the major constraints affecting the natural environment due to the associated environmental waste pollution. This constraint fostered the motivation to the present study, which reported on the findings obtained from the masonry bricks produced from blends of recycled crushed glass (RCG) and fly ash ( $\alpha$ -FA) with the inclusion of ordinary Portland cement (OPC) at varying percentages. The masonry bricks were produced with 5%, 10%, and 15% inclusion of OPC to the combined weight of  $\alpha$ -FA and RCG. The produced bricks rendered significant compression strength resistance compared to the fired clay bricks that are 3.8% higher on average. However, the compressive strength of all the produced bricks in this study satisfied the South African National Standard SANS 227 Code requirements (i.e.,  $\geq 7$  MPa) for individual load-bearing masonry brick. The scanning electron microscopy (SEM) analysis confirmed that the identified void spaces within the microstructure of the brick specimens with 5% OPC were the major cause of the low strength resulting from the incomplete pozzolanic reaction. Also, the effects of sulphate salt were significantly resisted on the surface of all the tested bricks incorporating  $\alpha$ -FA and RCG, due to the presents of aluminosilicates compounds that triggered pozzolanic reactions within the brick's matrix. The stiffness of the investigated bricks portrayed brittle characteristics due to the developed strength after production. This revealed the existence of a great proportionality between the dynamic modulus and ultrasonic pulse velocity (UPV) revealed a coefficient of determination ( $R^2$ ) equivalent to 90% because of the percentages of RCG particles.

**Keywords:** Masonry bricks, Dynamic modulus, Modulus of rupture, Waste, Sustainability.

## OPEN ACCESS

**Received:** May 20, 2021  
**Revised:** October 13, 2021  
**Accepted:** December 13, 2021

**Corresponding Author:**  
Aneke Frank Ikechukwu  
[AnekeF@ukzn.ac.za](mailto:AnekeF@ukzn.ac.za)

 **Copyright:** The Author(s). This is an open access article distributed under the terms of the [Creative Commons Attribution License \(CC BY 4.0\)](https://creativecommons.org/licenses/by/4.0/), which permits unrestricted distribution provided the original author and source are cited.

**Publisher:**  
[Chaoyang University of Technology](https://www.ijase.com)  
**ISSN:** 1727-2394 (Print)  
**ISSN:** 1727-7841 (Online)

## 1. INTRODUCTION

The upshoot in population has triggered more real estate developments which have extensively caused great utilization of soil deposit in brick production to a concerning level (Vosloo et al. 2016a). This reality has forced researchers and material scientists to shift their focus towards re-engineering, recycling, and remanufacturing of wastes from various sources.

One of the main wastes generated in South Africa is fly ash. It is generated from the burning of anthracite coal in power plants. Approximately, 250 Mt of coal in 13 power stations in South Africa are burnt by Eskom to generate 35,000 MW of electricity with 120.4 Mt of fly ash as the residual waste (Eskom, 2015).

Approximately 7% of this ash is supplied to the cement industry (Eskom, 2016; Laven et al. 2016). Currently, the availability of landfills for the disposal of this waste has become a challenge. However, fly ash obtained from the various power plant in South Africa are typical class “F” fly ash. This type of fly ash is required to be activated during soil stabilization hence the only suitable direct use masonry bricks production (Aneke and Awuzie, 2018).

Virtually all beverages and alcohol are sealed in a glass bottle. After consumption, these bottles are dumped in various landfills and recycled centres. However, the single-use purpose of glass bottles has resulted in generating millions of these wastes finding their way into landfills. Kaza et al. (2018) stated that waste glass contributes 5% to the total municipal solid waste generated globally, with the rate of recycling changing across regional lines. In the South African context, the recycling rate is equivalent to 40%, with 60% of the glass bottles being left in landfills and water bodies (CSIR, 2014). Furthermore, Europe recorded a glass recycling rate of 98%, in 2017 leaving European countries like Slovenia and Belgium contributing to 71.48% glass recycling rate. Furthermore, Turkey and the rest of the European countries recorded a glass recycling rate of 9% and 26.52% respectively (FEVE, 2019). In America, an average of 26.63% glass recycling rate was recorded in 2017, However, 52.9% of these glass containers generated are disposed of in the landfill (EPA, 2019). It is ascertained that the glass waste is non-biodegradable, as it abundantly fill-up valuable space in landfills. Thus, the dependency on natural resources is directly proportional to the rate of recycling practices which will ease off the burden on the depleting natural sources.

## 2. LITERATURE REVIEW

In the recent past, many studies have been seen focused on the use of waste materials as a partial replacement for natural clay in the production of bricks without compromising the strength as well as the durability of bricks (Aneke and Shabangu, 2021). In addition, several other studies (Velasco et al. 2014; Syed et al. 2016; Safeer et al 2017; Hasan et al. 2021; Shaqour et al. 2021) reported that the inclusion of recycled waste glass as a partial replacement of clay in brick production. These studies concluded that waste glass inclusion in bricks rendered higher strength associated with lower water absorption and apparent porosity due to decreased particle size of the glass. Furthermore, several studies published on partial replacement of clay with rice husk ash in brick production, have shown an increase in water absorption with decreased shrinkage and thermal conductivity (Kazmi et al. 2017).

Additionally, to reduce the embedded carbon footprint in construction materials, nanotechnology has also been applied for the production of masonry bricks. The nano application in bricks increases in compressive strength up to four times compared to fired clay bricks. However, the

setback on the application of nanotechnology in bricks production is that rigorous processes are required to transform the materials in nanosized scale as well as the sustainable and economical aspect of nanomaterials inclusion in brick production (Yehia et al. 2017). Wastes like marble and sawdust have been used in bricks production as well as other ceramic masonry residues. The inclusion of these additives contributes to decreasing in apparent porosity with relatively higher water absorption due to the nanosized particles of marble and sawdust. However, decreased porosity and compressive strength of the bricks produced with marble and sawdust could be mobilized with high sintering temperature (Sufian et al, 2021). It has been observed in past years that the construction industry is making a salient contribution towards saving the environment through recycling, remanufacturing, and reengineering of wastes. However, the most pronounced waste used in the production of low-cost construction material is fly ash. Other than the inclusion of fly ash in the production of construction materials, fly ash has a high value in subgrade stabilization (Aneke et al. 2015; Aneke et al. 2021). The quest to save the environment has compelled scientists to continuously research for an environmentally friendly material due to the dwindling non-replenishable natural materials. This quest has continued to propel the total conversion of waste for sustainable construction masonry bricks. Aneke and Shabangu (2021) developed a sustainable brick by using recycled crushed glass (RCG) and PET plastic waste to 100% waste masonry bricks without using any natural materials. Their result revealed that this type of PET waste bricks is 2.8 times stronger in strength and durability performance compared to fired clay bricks. In addition, the conversion of the PET waste and RCG to bricks reduced the production cost by up to 53% less because 22°C heat was required for production compared to fired clay bricks that require 1300°C what of heat for production. Liu et al. (2017) reported on the comparisons between red bricks and autoclaved aerated concrete (AAC) blocks. Their study concluded that AAC blocks reduced deadload from the wall on the beam by 20% and it caused a 50% reduction in cement consumption without compromising the strength. Aneke et al. 2021 explored the utility of waste foundry sand (WFS) and PET plastics blends in developing high-performance masonry bricks and their resistance in an acidic environment. From the foregoing, the utility of PET waste and WFS in facilitating industrial symbiosis within the construction industry and beyond, in general, and the housebuilding sector is no longer in doubt. As it has been elucidated in their study that the masonry bricks developed using these wastes possessed higher acidic and moisture resistance with associated high strength due to the hydrophobic properties of the parent waste.

This current study presents the use of  $\alpha$ -FA and RCG with various blends of OPC in the production of non-fired masonry bricks. Other than the significant strength and durability rendered by these bricks, this investigation also

suggested a novel approach towards reducing environmental pollution and landfill burden. Different mix ratio was designed for the bricks such as 70: 25: 5; 60: 30: 10; and 50: 35: 15 by the combined mass of  $\alpha$ -FA, RCG, and OPC to explore the effect these waste on different mechanical as well as durability properties of masonry bricks. Although, there are many existing studies regarding the utilization of fly ash in fired clay bricks; however, this investigation focused on the durability, compressive strength, modulus of rupture, static and dynamic modulus of non-fired waste bricks compressed with 20kPa after 12 h of production to compensate the environment as well develop a reliable balance between sustainability, economy, and energy-efficient of the bricks without severe threat on the environment.

### 3. STUDY SIGNIFICANCE

Clay is a naturally occurring material that is getting dwindled, due to the magnitude of utilization in the production of brick and cement-based materials. The usefulness of waste in South African towards curbing the incidence of lack of environmental pollution, lack of landfill space, development of low embedded CO<sub>2</sub> construction material remains largely underexplored. Fired clay bricks which happen to be prevalent in the construction of residential dwellings are prone to energy consumption with an associated threat to the natural environment. The high energy consumption levels often culminate in a significant increase in the CO<sub>2</sub> discharge to the environment thereby undermining the environmental integrity with a corresponding negative impact on climate change. With the increasing agitation for sustainable innovative and affordable housing in various countries, it has become imperative in South Africa to devise ways of dealing with the ever-increasing challenges of solving house shortages and effective waste management techniques that could reduce the threat and the burden on the natural sources for construction material. This is the gap which this study seeks to contribute towards bridging, as its central objective is to assess the utility of Fly ash and recycled crushed glass in tackling the challenges of the lack of affordable houses.

### 4. MATERIALS

The fly ash made available in this study was a typical class "F" fly ash obtained from the Lethabo power station in South Africa. According to the obtained X-ray fluorescence (XRF) result, it was revealed that the  $\alpha$ -FA possessed SiO<sub>2</sub>+Al<sub>2</sub>O<sub>3</sub>+FeO<sub>3</sub> above 70%. This indicated that the selected  $\alpha$ -FA is a typical class F fly ash in accordance with the standard specification for coal fly ash (ASTM C618, 2019).

The selected waste glass used herein was sampled from the Mariannhill landfill in Durban South Africa. The waste glass was crushed and graded into four particle sizes i.e.,

< 2 mm, 1-2 mm, 2-5 mm, 5-10 mm, and the oversized particles according to ASTM D1140 (2017) after collection. Based on the conducted pilot test, less than < 2 mm aggregate size of RCG was selected for this study due to the obtained ultimate strength in the produced bricks compared to other aggregate sizes as shown in Fig. 1. The recycled glass waste was from single sources including packaging bottles and jars.

The particle size of RCG is important because the number of voids between the particles influences the strength and microstructure of the bricks. The dominant chemical compositions in the RCG were evaluated to be SiO<sub>2</sub> with a dry mass of 64% and other trace chemical compositions such as Fe<sub>2</sub>O<sub>3</sub>, Al<sub>2</sub>O<sub>3</sub>, Cr<sub>2</sub>O<sub>3</sub>, and CaO making up the remaining 36% of the dry mass. The determination of different chemical compositions with their corresponding percentages was conducted using *X-ray fluorescence* equipment. This machine is of Rigaku, Ultima IV made with a diffractometer and a mounted Goniometer model 2036E201 operating with Cu K $\alpha$  radiation (K $\alpha$ =1.54056 Å) at an accelerating voltage of 40 kV and a current of 20 mA.

The OPC used in this investigation is Ordinary Portland cement (OPC) 42.5R, supplied by Lafarge cement South Africa. The cement was used in varying proportions as well as a binder in the production of non-fired masonry bricks.

The red silty soil used in this study was sampled from Pietermaritzburg South Africa. The red soil was used to produce fired clay bricks. Due to the possession of sufficient percentages of iron and aluminum oxides evaluated from the selected clay according to the XRF test. The clay material was certified suitable for brick production. Hence, Iron oxides exist mainly in the amorphous and crystalline inorganic forms. All the materials used in this investigation were oven-dried at a temperature 110°C for 24 hours, crushed, and sieved to the required particle size before bricks fabrication commenced. The specific gravity and chemical compositions of the materials obtained from XRF tests are summarized in Table 1.

### 5. PREPARATION OF THE BRICK SAMPLES

Fired clay bricks were produced in this study to eliminate any form of discrepancies that might influence the result from the non-uniformity of the bricks specimen. The clay material used for the production of these bricks is silty clay soil and the materials were mixed with water to the ratio of 2:1. The materials were thoroughly mixed using an automated mixer for 5 min prior to water addition. Afterward, the blends of the silty clay and water were further mixed for 10 min to ensure homogeneity of the material. Lumps of the mixture weighing 5 kg were placed in moulds sizes of 222 mm x 106 mm x 73 mm. The mould was thoroughly greased with a silicone spray to eliminate mixture adhesion to the walls of the mould. Confined pre-compression stress of 20kPa was uniformly applied on the

specimens after 12h of casting to eliminate void and increase the density of the bricks without any alteration on the brick size. The excess material was taken off using a spatula. Subsequently, the bricks were demoulded as a damp cloth was placed beneath the brick specimens covered with plastic bags prior to 3 days curing to prevent loss of moisture and carbonation. After drying, the bricks were moved and placed in a furnace capable of generating 1500°C of heat. Brick specimens were fired at a temperature of 1000°C for 48 h, after which they were placed on flat surfaces to cool for 2 days. Furthermore, the bricks were submerged in a curing bath for 28, 56, and 90 days, respectively for further curing.

The non-fired bricks were produced by blending fly ash with a recycled crushed glass of particles size of less than 2 mm. The varying percentages of  $\alpha$ -FA and RCG were

weighed out as 5%, 10%, and 15% of OPC were added to the dry mixture. The blend was thoroughly mixed for 5 mins under dry conditions and the missing continued for another 10 mins after water was added to obtain a homogeneous blend. Subsequently, the blend was cast into the mold and confined compression stress equivalent to 20 kPa was applied. Both the fired and non-fired bricks are presented in Fig. 2.

The bricks were demolded after 3 days of casting and were completely immersed in the curing bath for was 28, 56, and 90 days, respectively. A total of 75 bricks was produced for this investigation and the trial mix design of the bricks produced in this study is summarized in Table 2.

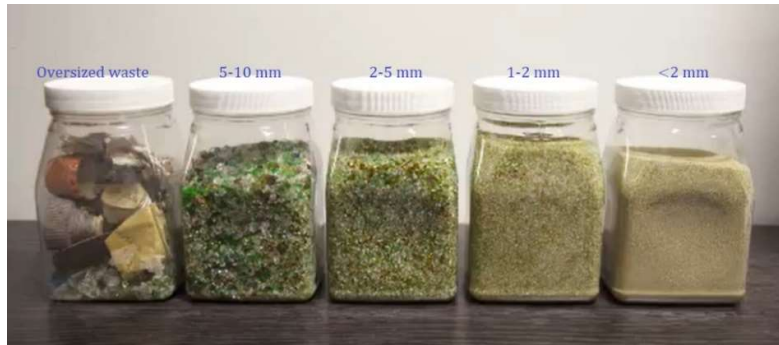


**Fig. 1.** Recycled crushed glass

**Table 1.** Chemical composition crushed glass.

Compounds	$\alpha$ -FA	RCG	OPC	Clay soil
SiO <sub>2</sub>	52.16	60.11	22.14	30.14
Al <sub>2</sub> O <sub>3</sub>	26.41	11.18	6.32	10.18
Fe <sub>2</sub> O <sub>3</sub>	11.09	7.26	4.17	40.11
CaO	3.62	3.78	64.23	6.12
MgO	5.55	0.22	2.15	4.40
Others	0.94	3.45	0.94	9.05
Specific gravity	2.75	2.9	3.10	2.84
Loss on Ignition (LOI)	0.23	0.084	0.055	0.012



**Fig. 2.** Showing fired bricks and non-fired bricks retrieved from the molds

**Table 2.** Materials mix proportion

Brick series	Clay (%)	OPC (%)	$\alpha$ -FA (%)	RCG (%)	W /M ratio	Mass (kg)
CB	100	-	-	-	2:1	3.2
NFB- 1	-	5	70	25	2:1	2.8
NFB- 2	-	10	60	30	2:1	3.0
NFB- 3	-	15	50	35	2:1	3.3

\*Clay brick \*\*NFB: None fired brick \*\*\* water-materials ratio.

## 6. EXPERIMENTAL METHODOLOGY

After the curing period, the produced brick specimens were retrieved from the water bath, cleaned with a dry cloth, and subjected to oven drying at 110°C for 24 h prior to testing. The compressive strength resistance (CSR) and modulus of rupture (MOR) tests were conducted following the ASTM C67 (2003) testing protocol. All the bricks were tested at a loading rate of 1.25 mm/min towards the direction depth. The modulus of rupture was conducted on the bricks in accordance with ASTM C583-15 (2021). The bricks were tested such that the span in between the supports was less than 40 mm of the brick's actual length. The load applied was administered at a rate of 1.25 mm/min in the direction of the brick's depth at the mid-span. A steel surface of 6 mm thickness and 40 mm width was placed at the top of the brick in the direction of the applied load. After the bricks specimen was fractured the distance between the line of fracture and nearest support was measured, and the modulus of rupture was computed using Equation (1).

$$\sigma_R = \frac{3PL}{2bd^2} \quad (1)$$

where  $\sigma_R$  is the modulus of rupture, P is the applied force, L is equal to the distance between the supported spans of the brick on the tension face, b and d are equivalent to the average width and depth of the bricks, respectively.

The durability studies of the bricks were conducted through the following tests: Initial rate of absorption, water absorption capacity, apparent porosity, and ultrasonic pulse velocity tests. The absorption capacity of the bricks was measured according to ASTM C67/ C67M (2020). Following the standard procedure, the brick specimens were first dried and weighed to determine the dry mass of the bricks. Afterward, the bricks were completely submerged in clean water at room temperature of 25°C for 24 h. Subsequently, the brick specimens were retrieved from the water bath and excess water from the surface of the bricks was wiped off and weighed again. The water absorption capacity of the bricks was determined using Equation (2).

$$W_a = \frac{M_2 - M_1}{M_1} \cdot 100 \quad (2)$$

where  $M_2$  is the wet mass of the bricks,  $M_1$  is equivalent to the dry mass of the bricks.

The apparent porosity of bricks was prescribed following ASTM C20 (2000) standard testing protocol for bricks. The bricks were submerged into boiling water for 2 h. Then

we're allowed to cool for 12 h until the hot water gets cold. The brick was then weighed while suspended in water, to measure the suspended weight and the saturated weight was also determined after cleaning the surfaces of the bricks with a dry cloth to remove excess water. The entire process was repeated three times before the average apparent porosity was determined using Equation (3). Again, the effect of apparent porosity on the compressive strength was evaluated, as each of the bricks was crushed after determining both the suspended and the saturated weight of the produced bricks.

$$P = \left( \frac{W - D}{W - S} \right) \cdot 100 \quad (3)$$

where P is the apparent porosity, W is the saturated weight, D and S are the dry weight and the suspended weight of the bricks, respectively.

Prior to durability testing, the bricks were left in the open air for 2 days under a constant temperature of 24°C. Followed by sulphate salt resistance test, this durability test was conducted according to ASTM C1012 (2018) procedures, as the bricks were fully submerged in different moles of 2.30E-05 M, 4.80E-06 M, 6.80E-07, and 8.80E-08 M of sodium sulphate per liter of water for 90 days. The bricks were dried at 110°C, weighed, and tested for compressive strength upon retrieved from the solution.

The ultrasonic pulse velocity (UPV) test was used to evaluate the flaws and homogeneity in brick specimens. The principle of the UPV test is to produce a pulse wave coming from the electro-acoustical transducer. The pulse wave is then transduced through the brick prism and the pulse wave time of travel through the bricks is measured. With the help of this time, the pulse velocity was evaluated. Two transducers were used, one is a transmitter, and the other is a receiver (Al-Nu'man et al. 2013). The UPV test was attained following ASTM C-597 as shown in Fig. 3. Ultrasonic Pulse velocity test equipment used in this study is equipped with a measuring range of 0–3000  $\mu$ s—accuracy  $\pm$ 0.1  $\mu$ s and two 55 kHz probes with connection cables. After the measuring exercise, the UPV was determined using Equation (4). Where the resonance frequency of the bricks specimens was recorded on the accelerometer on mechanical vibration using a claw hammer of 220 g.

$$V = \frac{L}{T} \quad (4)$$

where V is the ultrasonic pulse velocity, L is the distance between transducers and T is the transit time.



**Fig. 3.** Ultrasonic pulse velocity test setup for the brick specimen

## 7. RESULTS AND DISCUSSION

### 7.1 Compression Stress Resistance (CRS)

The compression stress resistance of the brick specimens is summarized in Fig. 4. The compression strength values reported in the curves were obtained from an average of 2 brick specimens with the mean value recorded as the final test results for 28 days, 56 days, and 90 days of curing period. The South African National Standards (SANS 2001.CM1: 2007) require minimum compressive strengths of 12.5 MPa after a 28-day curing period for double-story construction load-bearing masonry units. The NFB-2, NFB-3, and fired clay bricks specimens, cured at 28 days described in this study satisfied the SANS 2001.CM1: 2007 standards for compressive strength. The NFB-1 brick specimen failed to comply with the minimum required strength for the individual brick according to SABS 227 standard. The test results also revealed that the fired clay bricks rendered average compressive strength of 31.2 MPa before curing and 31.6 MPa value after 90 days of curing time. For non-fired bricks (NFB-1) the inclusion of 5% OPC triggered an average compressive strength of 8.1 MPa, whereas NFB 2 and 3 with 10% and 15% OPC content rendered average compressive strength of 19.3 MPa and 23.8 MPa respectively after 90 days of curing. Though the compressive strength result for individual bricks after 12 h of production without curing are 3.3 MPa, 6.25 MPa, and 10.38 MPa respectively for NFB-1, 2, and 3. Approximately 35.38% and 24.68% decrease in compressive strength was evaluated when the fired clay bricks are compared with NFB-1 and 2 respectively. A similar decrease in compressive strength was observed in NFB- 3 brick specimen as 18.92 % strength reduction was recorded compared to the fired clay bricks. Generally, the compressive strength of non-fired brick specimens increases exponentially as the curing time increase.

Whereas the fired clay bricks did not record any strength gain with curing time. The increase in strength was attributed to the pozzolanic reaction between OPC and  $\alpha$ -FA in the presence of available silica oxide from the RCG. Other than the inclusion of cementitious materials, dense density, low porosity, microstructure, and degree of applied pre-compressed stress during production contributed to high compressive strength according to (Eliche-Quesada et al. 2019).

Porosity is an important parameter that influences the strength of masonry bricks due to its effects on the brick's mechanical properties (Franzoni et al. 2015). A linear proportionality between compressive strength and apparent porosity of the produced brick was demonstrated in Fig. 5. The result revealed that a great proportionality exists between compressive strength and apparent porosity due to higher coefficient of determination ( $R^2$ ) values. The fired clay bricks in this study rendered an apparent porosity of 22% whereas NFB-1, 2, and 3 recorded apparent velocity values of 39%, 30%, and 26% respectively. The apparent porosity of the non-fired bricks in this study was low compared to the apparent porosity values of clay bricks. The result is consistent with the study published by (Sutas et al. 2018) which indicated that apparent porosity ranges between 35% - 45% due to the inclusion of waste sugarcane bagasse and rice husk ashes. However, the amount of silica present in bricks was related to the percentage contained in the RCG. Thus, the preferred percentage of silica for bricks ranges from 50–60%, beyond which the apparent porosity in the brick specimens will increase (Ukwatta et al. 2016). The content of silica in the RCG is within the acceptable percentage, therefore it mobilized the strength development and triggered a reduction in porosity. The increase in apparent porosity of the fired clay brick was due to the void space created by the sintering temperature during production causing defects within the burnt brick specimens (Yongue-Fouateu et al. 216).

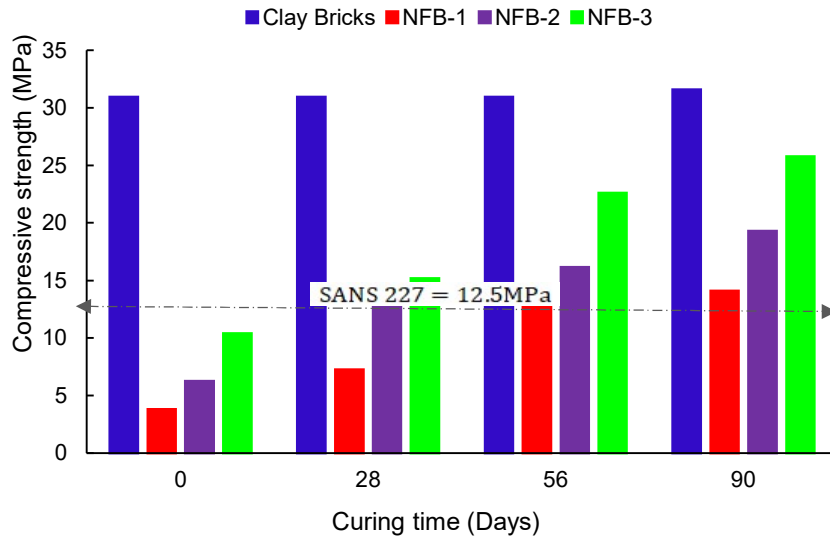


Fig. 4. Compressive strength of the brick specimens at various curing time

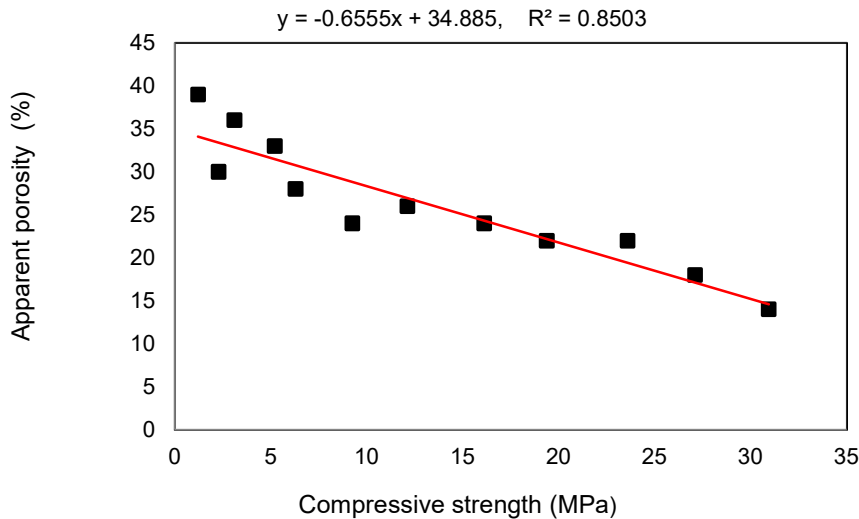


Fig. 5. Correlation of compressive strength with apparent porosity of the bricks

7.2 Modulus of Rupture (MOR)

Fig. 6 prescribed the modulus of rupture results for the fired clay bricks and non-fired brick specimens produced in this study. Results showed that the fired clay bricks recorded higher MOR values compared to the non-fired brick specimens. The maximum MOR value was observed for fired clay bricks is 1.7 MPa. However, the NFB rendered a significant modulus of rupture strength of 0.67MPa, 0.87 MPa, and 0.96 MPa for NFB-1, 2, and 3 after 90 days of curing time. The variation in modulus of rupture strength was noted to be consistent with OPC dosage. However, an average 34.3% decrease in MOR value was observed for NFB compared to the fired clay bricks. This response in MOR value for NF bricks agrees with the previous study

published (Naik et al. 2014) which concluded that the inclusion of cement triggered a significant increase in MOR value. It was observed that the brick modulus of rupture is relative to the microstructure of the brick specimens. Thus, the inclusion of RCG and  $\alpha$ -FA triggered increased the modulus of rupture strength that is mobilized by the tightly knitted porous structures for the NF bricks. The allowable value of MOR is 0.65 MPa according to (ASTM C67,2003a). All the non-fired brick specimens exhibited MOR values in the range of 0.67–1.7 MPa except for NFB-1 with a MOR value of 0.42 MPa. Therefore, this result implies that more than 5% of OPC is required to produce bricks with acceptable mechanical properties.

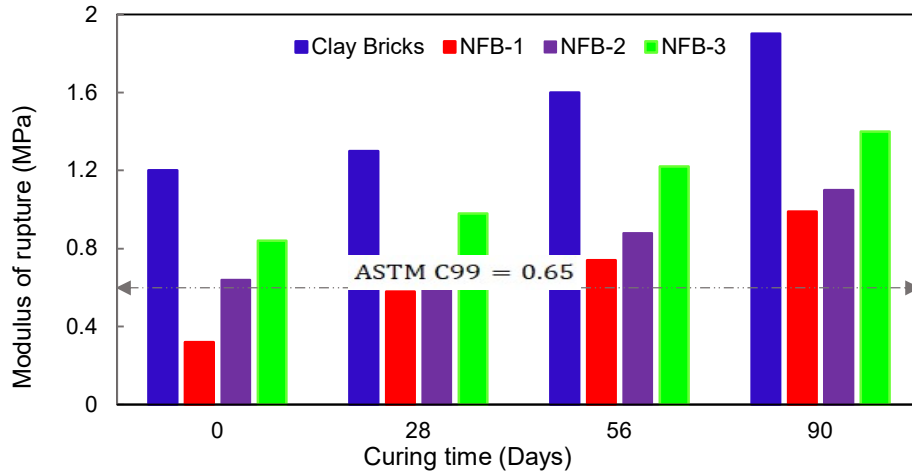


Fig. 6. Modulus of rupture strength of the brick specimens at various curing time

7.3 Correlation of CSR with MOR of the Bricks

The correlation between the CSR and MOR of bricks-fired clay and non-fired bricks is presented in Fig. 7a and Fig. b. It is ascertained that the flexural strength of the fired clay bricks compressive strength value is 6 times higher than its MOR value. This implies that the fired clay bricks could withstand bending failures compared to the non-fired bricks. Yu and Park (2021) stated that the reinforced bricks unit is designed to carry compressive as well as tensile stresses. However, the relationship between the compressive strength and MOR is a strength index used to measure the flexural competence of construction materials. However, a bi-linear proportionality exists between the CSR and MOR of all the tested bricks. This proportionality resulted in a coefficient of determination (R2) values of 93%, 94%, 96%, and 85% respectively fired clay bricks, NFB 3, 2, and 1. The higher percentages of R2 indicated that the bricks possess sufficient strength for load-bearing masonry structural units. However, the strength is directly proportional to the percentages of recycled crushed glass,  $\alpha$ -FA, OPC, precompressed stress, and brick porosity. The ratio of MOR to the compressive strength of concrete is 10% on average. Whereas a 9.34% ratio of tensile strength to compressive strength expressed was obtained in this study. It can be concluded that the produced masonry bricks in this study could sustain flexural stress as a masonry unit. Though, factors like, type of mortar, mortar materials, and the direction of loading could influence the flexural tensile strength in a masonry unit. Thus, the individual flexural tensile strength of brick contributes to 65 to 70% of the flexural strength (McCormac and Brown, 2015).

7.4 Stress-Strain Failure Response of Bricks

The stress-strain response of the fire-clay bricks and non-fired bricks cured for 90 days is shown in Fig. 8. It was observed that the fired-clay bricks specimens exhibited high stiffness when under compression. Though lesser stiffness

response was observed for the non-fire bricks specimens compared to the fired clay bricks. The clay bricks are associated with brittle compression failure at a strain value of 0.04 and 0.05. The behaviour was observed immediately after the elastic zone, this could be evidenced after the peak load. The stress-strain behaviour of the non-fired bricks under compression is characterized by a linear proportionality within the deformation strain of 0.02 to 0.04, beyond which strain hardening occurs. However, both the fired and non-fired bricks portrayed brittleness response, hence slight post-peak ductile behaviour was observed particularly on the bricks that contain recycled crushed glass. The compression failure mode for non-fired bricks is characterized by specimens’ crushing whereas fired-clay bricks specimens show multiple planes of failure. It is worthy to mention that the material relaxation might have been triggered by the RCG content and microstructure arrangement of the non-fired bricks. The stress-strain characteristics of bricks do not behave elastically even in the range of small deformations due to the brittleness of the bricks (Stefanidou et al. 2015).

The method of static equilibrium was used to determine the elastic properties of bricks produced herein. The brick was subjected to compression load in the direction perpendicular to the planes of bedding. However, the longitudinal compressive strain ( $\epsilon_y$ ) and the corresponding lateral tensile strain ( $\epsilon_x$ ) were measured from the electrical strain gauges mounted in both directions of forces. The load-deformation was converted to stress and the stress-strain curve data was obtained from the data logger. From the plotted stress-strain curve, the Young modulus (E) and Poisson’s ratio ( $\mu$ ) were obtained from the slopes of the linear portions of the legends using Equation (5) and (6).

$$E = \frac{\sigma_y}{\epsilon_x} \tag{5}$$

$$\mu = \frac{\varepsilon_x}{\varepsilon_y} = \frac{\sigma_y/\varepsilon_y}{\sigma_x/\varepsilon_x} \quad (6)$$

where E is the young modulus,  $\mu$  is the Poisson's ratio,  $\sigma_y$  is the stress in the y-direction,  $\varepsilon_x$  and  $\varepsilon_y$  are the lateral

tensile strain with the corresponding longitudinal compressive strain, respectively.

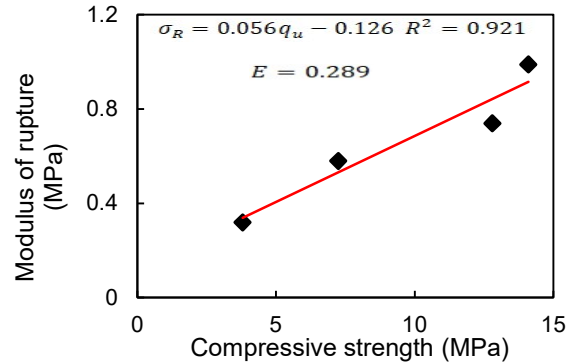
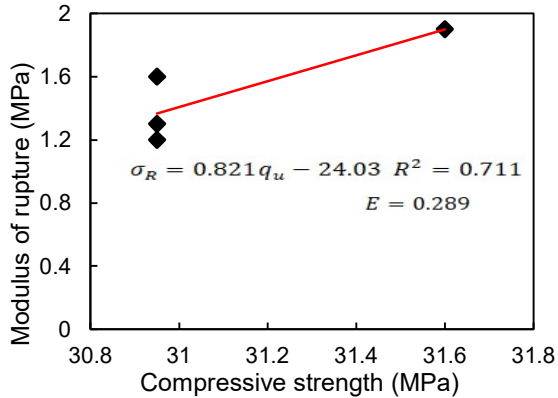


Fig. 7a. Correlation of CSR with MOR of the fired-clay bricks and NFB-1

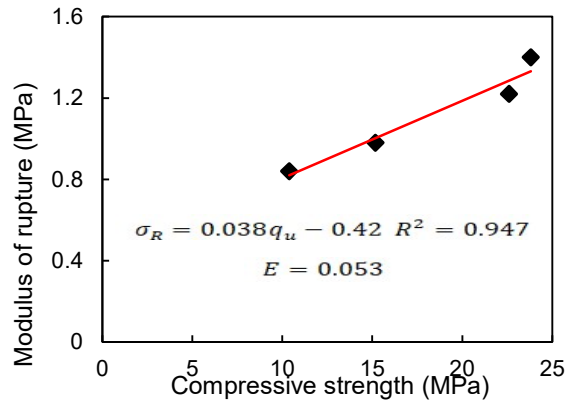
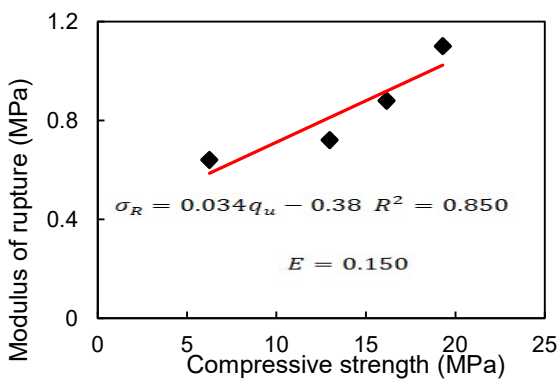


Fig. 7b. Correlation of CSR with MOR of the NFB-2 and NFB-3

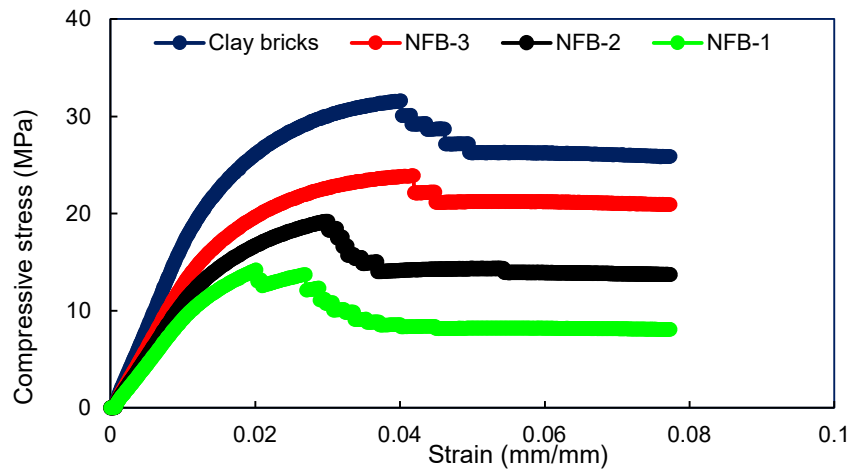


Fig. 8. Stress-strain variation of bricks

## 8. DURABILITY PROPERTIES OF BRICK SPECIMENS

### 8.1 Initial Rate of Absorption (IRA)

The IRA of the investigated bricks is presented in Fig. 9. The IRA result for the fired clay bricks in this study was evaluated to be 25 g/m<sup>2</sup>/min. Similarly, NFB-1, 2, and 3 rendered IRA values of 45 g/m<sup>2</sup>/min, 29.57 g/m<sup>2</sup>/min, and 27 g/m<sup>2</sup>/min, respectively. According to ASTM C67 (2020), for a brick to provide good bond strength with mortar, it should have a minimum IRA value within the range of 25 to 30 g/m<sup>2</sup>/min. Thus, with an IRA value higher than 30 g/m<sup>2</sup>/min, it implies that the brick units are highly absorptive and should be wetted prior to laying to achieve adequate bond strength. However, these IRA limit values were derived based on tests carried out on clay bricks. Basha and Kaushik (2014) reported that the IRA values for fly ash bricks vary from 35 to 50 g/m<sup>2</sup>/min with an average of 40 g/m<sup>2</sup>/min. It is also indicated that the blends, of fly ash and RCG in bricks produced in this study could be used as an alternative to clay brick without any need for pre-wetting. However, it could be understood that the value of IRA is found to be higher in non-fired bricks compared to fired clay brick. Thus, the IRA gives an insight into the pre-wetting time needed and bond strength of brick masonry. It was noted that the initial rate of absorption for brick specimens incorporating fly ash and RCG were higher compared to that of fired clay bricks.

### 8.2 Relationship Between Water Absorption and Apparent Porosity of the Bricks

The absorption of water in masonry bricks is one of the major factors that affect bricks' durability (Aakash and Devendra, 2014). It is noted that the correlation of water absorption with apparent porosity of the bricks produced herein rendered a high correlation coefficient R<sup>2</sup> of 0.865 as shown in Fig. 10. This indicates a great proportionality between the two durability parameters due to the existing porosity within the brick's specimens. It was noted that the water absorption capacity of the fired clay bricks is slightly low compared to the NFB-3 that contained varying proportions of  $\alpha$ -FA, RCG, and OPC. For instance, NFB-1 which contained 5% of OPC, 70%  $\alpha$ -FA, and 25% RCG recorded water absorption of 11.52%; while NFB-2 with 10% of OPC, 60%  $\alpha$ -FA, and 30% RCG rendered a water absorption value of 13.12%. Similarly, 18.28% and 12.31% values of water absorption were obtained for NFB-3 which contained 15% of OPC, 50%  $\alpha$ -FA, and 35% RCG as well as fired-clay bricks, respectively. It is worthy to mention that the NFB-1 specimens with 70% of  $\alpha$ -FA are associated with the highest water absorption capacity. This can be attributed to the increasing percentage of  $\alpha$ -FA content in the bricks hence with a higher percentage of  $\alpha$ -FA more water is required to complete the pozzolanic reaction. The water absorption and apparent porosity portrayed a linear relationship due to the great proportionality between  $\alpha$ -FA

content and the porosity of the bricks (Arati, 2016). In reference to ASTM C62 which stated that a maximum of 17% of water absorption is allowed in bricks for severe weathering resistance hence 22% is recommended for moderate weathering. Based on the available literature, water absorption limits for  $\alpha$ -FA brick specimens ranges from 20% to 30% (Prabhat et al. 2019). Water absorption was approximately 22%, 18.12%, and 15.28% for NFB-1, 2, and 3, respectively. Thus, the result implies that NFB-1 is suitable for construction in moderate weather regions. Whereas, the fired clay bricks, NFB-2, and 3 are more suitable for construction in severe weathering regions. It could be concluded that the inclusion of  $\alpha$ -FA, RCG, and OPC in bricks production is within the specified limits of water absorption leading to cost-effective and durable masonry construction.

### 8.3 Bricks Resistance to Sulphate Salt

Salts like sodium chloride (NaCl) and calcium sulphate (CaSO<sub>4</sub>) are usually present in bricks. The manifestation of these salts is usually from different sources such as groundwater, rainwater, mortar, and improper use of chemical cleaners. Previous studies have ascertained that NaCl salt usually migrates from mortar joints when NaCl is used as an accelerator. More so, NaCl could also manifest on the surface of the brick through the contamination of masonry units (Balksten and Strandberg-de Bruijn, 2021). However, all salts do not have structural implication damage, except Na<sub>2</sub>SO<sub>4</sub> and NaCl, thus these salts are significantly resisted by bricks with sufficient fly ash content (Granneman et al. 2019).

The fired clay bricks showed low resistance against sulphate salt, this caused a decrease in compressive strength as presented in Fig. 11. The strength reduction in the fired clay bricks is approximately 12.25%. Whereas strength reduction rendered by non-fired bricks was in the range of 5% to 9%, depending on the percentages of  $\alpha$ -FA and RCG. The reduction in compressive strength for the fired clay bricks is relative to the precipitate generated through the crystallization of sulphate salts within the micro-pores of the bricks, as it triggered internal micro-cracking within the bricks. In addition, it was observed that the non-fired bricks portrayed strong sulphate resistance as compared to fired clay bricks due to the hydrophobic property of RCG contents that prevents NaCl salt solution from permeating the bricks pores space. In Table 3, the results also showed that weight gain in the fired clay bricks was around 15%, whereas it ranged from 3 % to 6% for the non-fired clay bricks with various content of  $\alpha$ -FA, RCG, and OPC. The weight gain was due to the partial infiltration of NaCl salt crystals within the brick's spaces (Naik et al 2014). Based on the results, it is evident that non-fired bricks produced with different contents of  $\alpha$ -FA, RCG, and OPC provides strong resistance against sulphate salt attack.

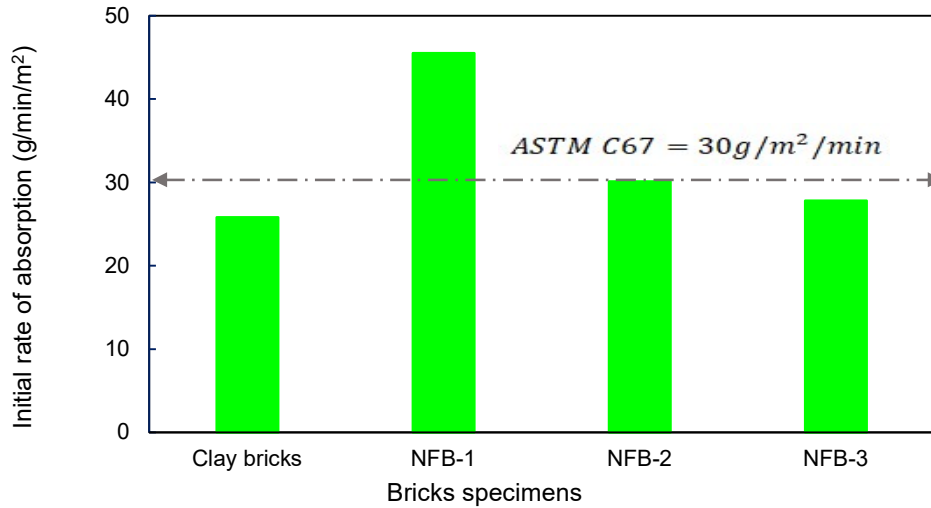


Fig. 9. Initial rate of absorption for the produced brick specimens

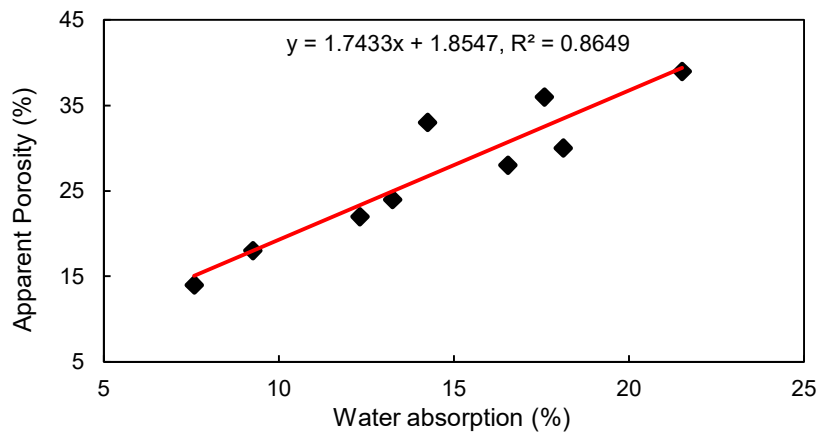


Fig. 10. The proportionality of water absorption with apparent porosity of the bricks

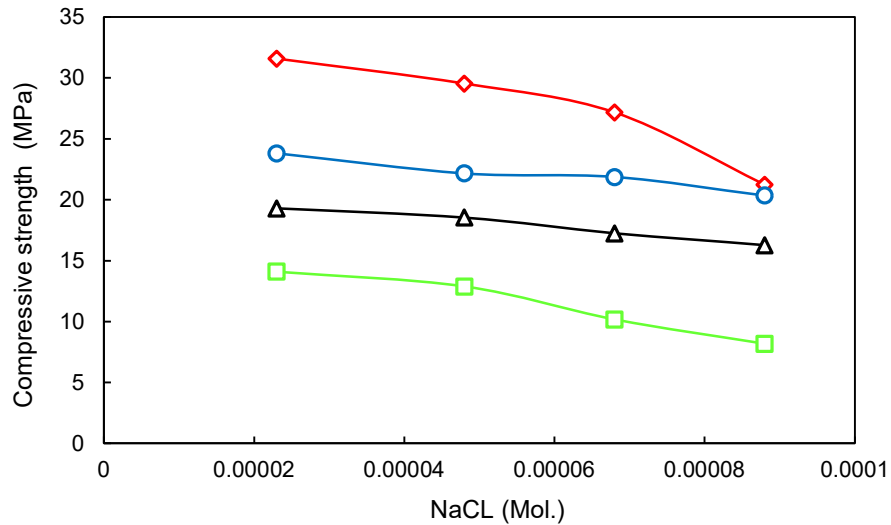


Fig. 11. Bricks response to sulphate salt solution

**Table 3.** Bricks acidic submersion

Series	Molarities (M)	Initial strength (MPa)	Strength decrease (MPa)	Strength decrease (%)
Clays bricks	2.30E-05	31.60	21.25	32.75
	4.80E-06	31.60	27.17	14.02
	6.80E-07	31.60	29.54	6.52
	8.80E-08	31.60	31.25	4.27
NFB-1	2.30E-05	14.10	8.18	41.99
	4.80E-06	14.10	10.18	27.80
	6.80E-07	14.10	12.88	8.65
	8.80E-08	14.10	13.95	1.06
NFB-2	2.30E-05	19.30	16.28	15.65
	4.80E-06	19.30	17.25	10.62
	6.80E-07	19.30	18.54	3.94
	8.80E-08	19.30	18.92	1.98
NFB-3	2.30E-05	23.80	20.35	14.50
	4.80E-06	23.80	21.87	8.11
	6.80E-07	23.80	22.17	6.85
	8.80E-08	23.80	23.80	-

8.4 Ultrasonic Pulse Velocity of the Bricks

The Ultrasonic pulse velocity evaluates the homogeneity of brick’s quality. The brick quality is a very noted parameter in every construction, as such the quality of bricks investigated herein was determined through the ultrasonic pulse velocity testing method. Pravez et al. (2021) in their research concluded that the UPV test is reliable in detecting detect flaws as well as predicting the compressive strength of bricks. The uniformity of the bricks was evaluated using UPV as illustrated in Fig. 12. It was found that NFB-1, 2, and 3 yielded lower UPV values compared to that of fired-clay bricks before curing commenced. However, the UPV values for NFB-1, 2, and 3 bricks increased exponentially from 1845m/s to 3248m/s from 28 days to 90 days on average. Whereas the UPV values for fired clay bricks increased from 3683 m/s to 3795 m/s. Moreover, no further increase in UPV values was recorded for the fired clay bricks as the curing time increased. Generally, UPV values increase as strength increased. The UPV test results obtained in this study have similar consistency with the bricks’ compressive strength values. Based on the previous studies by (Sarkar and Faris, (2019), a is bricks certified suitable if their UPV is greater than 3500 m/s and non-suitable for UPV values less than 1000 m/s. Therefore, the UPV values for all the tested brick specimens ranged from 1800 to 3500 m/s, and investigated bricks are certified durable based on the obtained UPV values. The obtained values could be attributed to the pre-compressed pressure applied on the bricks, microstructure, porosity, and the developed pozzolanic reaction during the curing period.

8.5 Correlation Between Dynamic of Modulus ( $E_d$ ) and UPV

The elasticity modulus of bricks is a fundamental parameter that characterizes the deformation response of masonry brick in compression. Thus, it is the most relevant material property relative to stiffness. In addition, the

dynamic modulus ( $E_d$ ) is the ratio of stress to strain under vibratory conditions and it is the property of viscoelastic materials. The dynamic modulus could be calculated either through the static or dynamic method. The former involves direct loading of a specimen and measuring the corresponding change in the strain as the stress is applied. The static elastic modulus is then computed by evaluating the slope of the experimental stress-strain curve in the elastic deformation range. On the other hand, the  $E_d$  was evaluated through pulse waves using Equation (7) and (8) according to ASTM C-597 (2016) protocol. Hence the  $E_d$  of the brick specimens produced in this study was calculated by substituting the values of density, UPV, and poisons ratio. To quantify the dynamic performance of the bricks, the dynamic modulus of elasticity was correlated with UPV for both fired-clay bricks and non-fired bricks as shown in Fig. 13.

$$V = \sqrt{\frac{E_d(1 - \mu)}{\rho(1 + \mu)(1 - 2\mu)}} \tag{7}$$

$$E_d = \frac{V^2[\rho(1 + \mu)(1 - 2\mu)]}{(1 - \mu)} \tag{8}$$

Where  $E_d$  is the dynamic modulus of elasticity,  $V$  is the ultrasonic pulse velocity test of the bricks,  $\rho$  is the density at 90 days curing,  $\mu$  is the Poisson’s ratio obtained from the stress-strain graph in Fig. 8.

The  $E_d$  value of the fired-clay bricks is higher compared to the non-fired bricks. The  $E_d$  value for the fired-clay bricks at 28 days is 21 GPa, thus this value increased exponentially to 33 GPa at 90 days of curing time. On the order hand, the dynamic modulus value of NFB-1, 2, and 3 ranges from 12 GPa to 22 GPa for 28 and 90 days. The correlation between  $E_d$  of elasticity and UPV of bricks showed a higher coefficient of determination of 90%, indicating a great proportionality between dynamic modulus and UPV. The  $E_d$  values of all the bricks investigated in this study

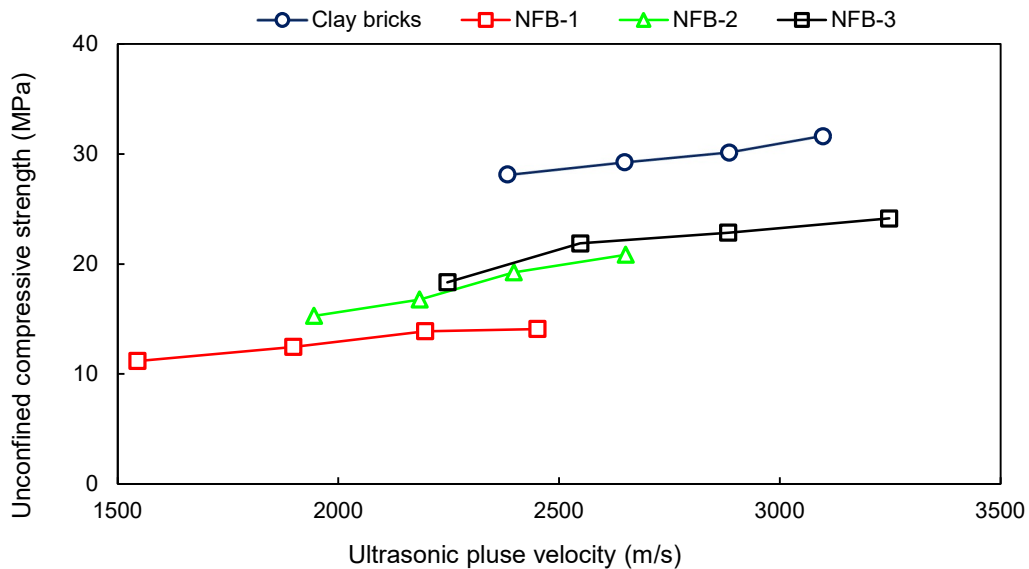


Fig. 12. Ultrasonic pulse velocity test for produced bricks

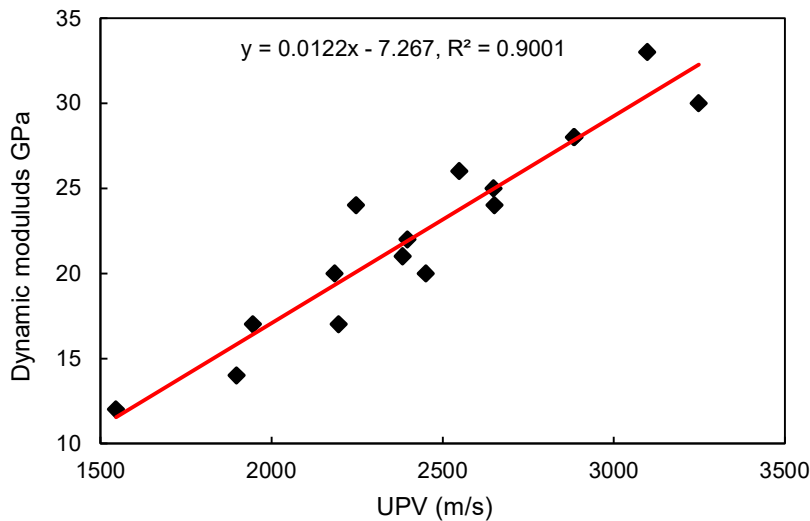


Fig. 13. The relationship between dynamic modulus of elasticity and UPV of the bricks

imply that the bricks specimens are homogeneous.

This result could be attributed to the microstructure, precompression applied pressure during brick production, and less apparent porosity values of the fired-clay bricks compared to non-fired bricks. However, NFB-3 after 90 days of curing portrayed a stiffer elastic behaviour than NFB-1 and 2. Generally, it was observed dynamic modulus of elasticity of the fired clay bricks is higher compared to the non-fired clay bricks. This was expected due to the higher quality and less porous of the fired clay bricks compared to the non-fired bricks, therefore they exhibit a stiffer elastic behaviour as confirmed by the stress-strain curve (Fei et al. 2016).

## 9. MORPHOLOGICAL STUDY

The microstructure of the investigated bricks was accessed through scanning electron microscopy (SEM) as presented in Fig. 14a, b, c, and d. The micrograph showed irregular shapes of clay minerals knitted as a matrix due to firing temperature, indicating the presence of the following crystalline phases: quartz, Kaolinite, celadonite, and hematite. It was observed that quartz and glauconite were dominant at the crystalline phase. Whereas NFB-1, 2, and 3 are comprised of quartz in excess due to increasing percentages of recycled crushed glass. In furtherance, the discrete presence of mullite, hematite, maghemite, and anhydrite, were also identified beyond trace level on the

microphase of the non-fired bricks. The micrograph showed cementitious compounds because of pozzolanic reaction between OPC, RCG, and  $\alpha$ -FA characterized with flocculated arrangements and has fine crystalline like-structures within the brick's matrix. The SEM micrographs exposed scales of observation and the dominant features of the microstructure of fired-clay bricks and non-fired bricks. Both microstructures converge to a common pattern at larger scales of the non-fired bricks. Thus, few cementitious minerals were identified on the micrograph fired-clay bricks due to the degree of temperature to crystalline microstructure. The non-bricks were also transformed from amorphous phase to crystalline phase due to the curing period as the bricks are characterized by a different type of matrix phase which hosts few mineral components for strength development. More specifically, the matrix of NFB-3 is a composite of amorphous glass, crystals of primary mullite, and occasional acicular forms of secondary mullite as the curing age increases forming a spinel-type phase which was identified as hematite.

## 10. SUSTAINABILITY AND CO<sub>2</sub> EMBODIMENT ANALYSIS OF FLY ASH BRICKS

The sustainability analysis was achieved through a CO<sub>2</sub> emission comparison between the fired clay and non-fired bricks relative to material cost production and sustainability. To quantify the CO<sub>2</sub> embodiment of both the fired-clay and non-fired fly ash bricks, the cost of energy production of these bricks was carried out using a 2-bedroom masonry structure as a case study. The mix formulation used in the production of both fired and non-fired bricks is presented earlier in section 5. However, it is presumed that cost of extraction, sorting out and transportation of clay, fly ash, and recycled crushed glass is the same, therefore these costs were not considered in this analysis. The cost of energy production invested in the production process of these bricks for the construction of a 2-bedroom masonry structure was demonstrated using CO<sub>2</sub> embodiment as a function of sustainability and green-efficient indices. Hence the same quantity of mortar will be required for the masonry construction for both the fired clay brick and non-fired bricks. Therefore, the energy cost of mortar is excluded in this analysis.

The energy cost of electricity for households and businesses which includes all components of the electricity bill such as the cost of power distribution and taxes according to Eskom (2009) is R2.38 and R1.83 Rands per kWh. This is equivalent to 0.145 US and 0.070 US dollars per kWh. Therefore, 1 kWh of electricity is equivalent to 1895.63°C of heat. Based on the calculation analysis performed in this study, it will require 0.58 kWh to generate 1100°C worth of heat to produce 1 fired clay brick unit.

Whereas 0.76kWh is required to generate 1450°C worth of heat to produce 1 ton of cement production is a thermal energy-intensive process. However, 15% of the cement used to produce the bricks used in this study is equivalent to 0.114kWh of energy used for the production of the non-fired fly ash bricks. Considering the energy production cost for fired clay bricks, the cost for 1 brick unit is R1.38 (R2.38 x 0.58kWh) while the non-fired fly ash brick cost is R 0.271 (R2.38 x 0.114kWh). To evaluate the quantities of CO<sub>2</sub> embodiment for both the production of fired clay and non-fired fly ash bricks, coal-based power plants are used in South Africa, hence the power plants emit an average of 915 grams of carbon dioxide (CO<sub>2</sub>) per kilowatt-hour of electricity produced. It has been calculated that 0.58 kWh and 0.114 kWh electricity are required to produce 1 unit of both fired clay and non-fired fly ash bricks, respectively. Therefore, to calculate the quantities of CO<sub>2</sub> emission for clay brick, (915 g x 0.58 kWh) 531 g of CO<sub>2</sub> will be emitted into the environment, whereas (915 g x 0.114 kWh) 104 g of CO<sub>2</sub> will be discharged into the environment to produce non-fired fly ash bricks. It is worthy to note that 104 g of CO<sub>2</sub> is the emission generated from cement production. According to the calculated bill of material quantity presented in this study, it requires 23534 pieces of bricks for the construction of a two-room masonry structure of 20 m in length, 3 m width, and 4 m height, using double leaf wall with the exclusion of 2 doors and 2 windows spaces. Each brick weighs an average of 3.3 kg, therefore it required (23543 x 3.3) 77662.2 kg of clay to produce 23534 pieces of clay bricks. Therefore, the total quantities of CO<sub>2</sub> in kilograms that will be discharged into the environment for the construction of a 2-bedroom masonry structure are (0.531 kg x 77662.2 kg) 41239 kg worth of CO<sub>2</sub>. To calculate the quantities of CO<sub>2</sub> embodiment for the production of non-fired fly ash bricks in kilogram, hence 50% of fly ash waste inclusion rendered the ultimate strength therefore the quantities of material required for the construction of 2-bedroom masonry structure will be 50% multiplied by the quantities of material required for the construction multiply by the quantity of CO<sub>2</sub> emission required for a single unit of fly ash bricks (0.5 x 77662.2 kg x 0.104 kg) and this corresponds to 4038.43 kg of CO<sub>2</sub> emission. The summary of the estimation of the bricks quantity of CO<sub>2</sub> emission is presented in Table 4. It is worthy to mention that the calculated CO<sub>2</sub> emission for both fired clay and non-fired fly ash bricks is based on the kilograms of energy required and CO<sub>2</sub> embodiment cost to produce these bricks. Using the information provided in Table 4, it follows that over (0.5 x 77662.2 kg) 38831kg of fly ash waste is saved from stockpiling in the landfills, compared to about 77662.2 kg of natural clay required for the construction of a two-room structure, with a consequent saving of (41239-4038.43) kg = 37201 kg of carbon dioxide.

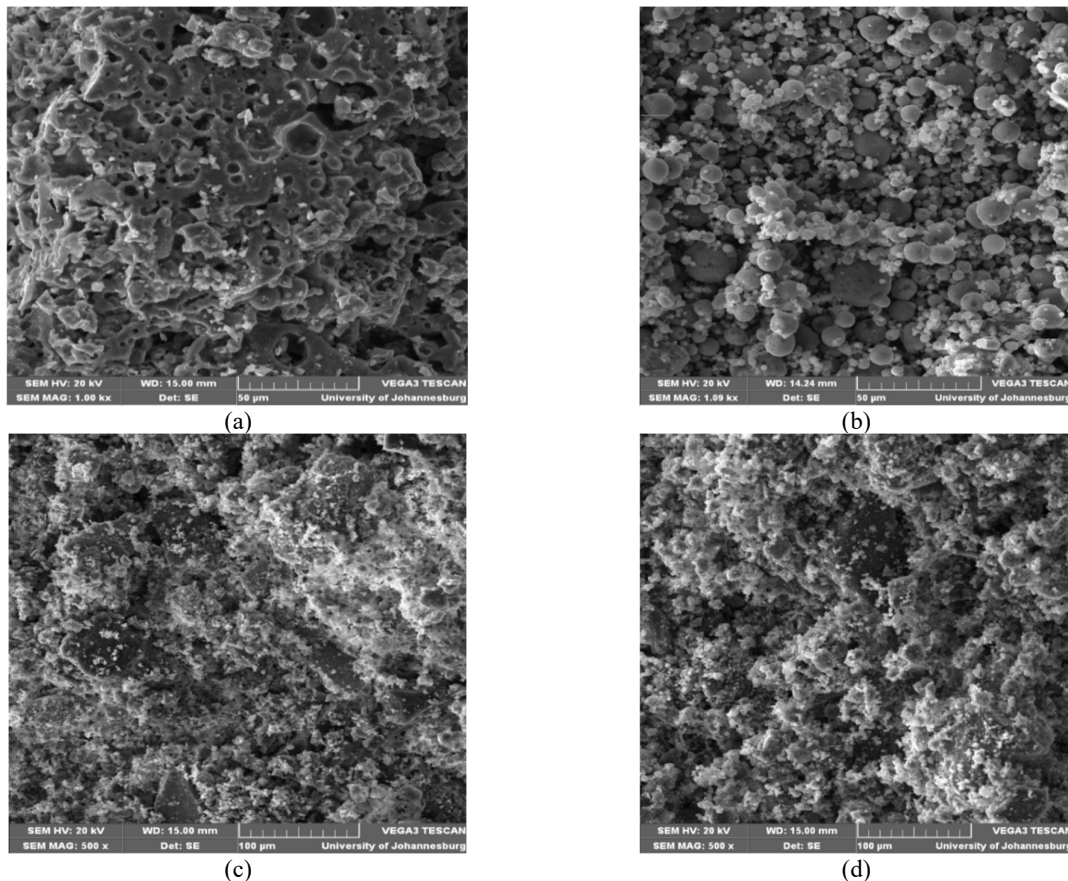


Fig. 14 (a). Micrograph of fired clay, (b). (c) and (d). Micrograph of NFB-1, 2, 3 and 4

Table 4. Bricks sustainable and embedded CO<sub>2</sub> analysis

Bricks	Heat (°C)	Production Time (Minutes)	Average Density (kg/m <sup>3</sup> )	CO <sub>2</sub> Emission (kg)	Price/energy cost	Sustainability
NFB- 1	725	15 – 20	3645.8	5654	R 0.271/brick	Favorable
NFB- 2	725	15 – 20	3906.3	4846	R 0.271/brick	Favorable
NFB- 3	725	15 – 20	4296.9	4038	R 0.271/brick	Favorable
Clay bricks	1100	3 -6 day	4172	41239	R 1.34/brick	Not Favorable

## 11. CONCLUSIONS

In this research, the inclusion of  $\alpha$ -FA and RCG in brick production has been studied through the indices of strength and durability. The inclusion of these wastes in masonry bricks could be considered cost-effective as well as conserving dwindling natural clay material toward the production of sustainable, green-efficient, and re-engineering of wastes.

The properties of masonry bricks produced with  $\alpha$ -FA, RCG, and OPC were investigated in this study. The utilization of fly ash and RCG wastes as a raw material in the manufacturing of non-fired bricks is one of the rational ways of recycling abundant wastes, leading to conservation space including water and soil. The  $\alpha$ -FA and RCG used in

this study were abundantly waste materials, having a high percentage of crystalline silica that possess the properties of filler material.

The utilization of  $\alpha$ -FA and RCG with varying percentages of OPC is proven in this study as resourceful material for non-load bearing bricks for masonry construction. The bricks also portrayed great potentiality against dynamics stress due it high values of dynamic modulus. It was observed that the blend of 50%  $\alpha$ -FA, 35% RCG, and 15% OPC of non-fired bricks resulted in 25.8 MPa with approximately 25.19% and 82.9% increase in strength compared to NFB-1 and 2, respectively. These compressive strength values of the non-fired bricks satisfy the requirement of compressive strength specified by South African standard specification for burnt clay masonry units

(SANS 227, 2007), which requires nominal compressive strength for face bricks to be greater than 17.0 MPa, with individual strengths greater than 12.5 MPa, for burnt clay brick with a loadbearing capacity of retaining walls and story buildings. This low compressive strength resistance values recorded for NFB-1 and 2 bricks specimens are mobilized by low OPC and  $\alpha$ -FA, hence failing to meet the minimum required strength as stipulated by SANS 227, 2007.

Resistance against sulphate attack is recommendable for the NFB-1, 2, and 3, indicating their suitability in sulphate salt environments due to their high resistance capacity. It was found that UPV values of the bricks complied with compressive strength resistance and bricks homogeneity. A great correlation between the dynamic modulus and UPV is mobilized by the homogeneous characteristics of all the tested bricks which implies that dynamic modulus increases with an increase in UPV.

Furthermore, it was observed that the apparent porosity of the NFB-3 increased with a higher percentage of OPC which triggered an increase in water absorption compared to fired clay bricks. The NFB-1 showed the highest water absorption among all the produced bricks in this study due to the high content of  $\alpha$ -FA, which requires more water for a complete pozzolanic reaction. The SEM revealed that the microstructure of the brick specimens hence NFB-1 is mobilized with a higher initial rate of absorption of 30 g/m<sup>2</sup>/min. Therefore, the NFB-1 requires completely submerged in water prior to its use in masonry construction.

## ACKNOWLEDGMENT

The author's acknowledgment goes to the Geotechnical and Materials research group at the University of Kwazulu-Natal Durban, South Africa.

## DECLARATION

There is no known form of conflict of interest as regards this manuscript.

## DATA AVAILABILITY STATEMENT

Please, note that all data, models, and code generated or used during the study appear in the submitted article.

## REFERENCES

Aakash, D.P., Devendra, B.G. 2018. Engineering properties of clay bricks with the use of fly ash. *Int. J. Res. Eng. Technol.* 03, 75–80 Google Scholar  
Al-Nu'man, B.S., Aziz, B.R., Abdulla, S.A., Khaleel, S.E. 2015. Compressive Strength Formula for Concrete using Ultrasonic Pulse Velocity. *Int. J. Eng. Trends Technol. IJETT* 2015, 26, 8–13

Aneke FI, Okonta FN and Ntuli F. 2015. Geotechnical Properties of Marginal Highway Backfill Stabilized with Activated Fly Ash Msc Thesis, Dep. Of Civil Eng. Sci. And Built Envir. University of Johannesburg, Gauteng, South Africa.  
Aneke, F.I., Awuzie, B. 2018. Conversion of industrial wastes into marginal construction materials, *Acta Structilia*, 25 2, 119–137, 10.18820/8820/24150487/as25i2.5  
Aneke, F.I., Shabangu, C. 2021. Green-efficient masonry bricks produced from scrap plastic waste and foundry sand, *Case Studies in Construction Materials*, Volume 14, 2021, e00515, ISSN 2214–5095, <https://doi.org/10.1016/j.cscm.2021.e00515>  
Aneke, F. I, Shabangu, C. 2021. Strength and durability performance of masonry bricks produced with crushed glass and melted PET plastics, *Case Studies in Construction Materials*, 14, 2021, e00542, ISSN 2214–5095, <https://doi.org/10.1016/j.cscm.2021.e00542>  
Aneke, F.I., Awuzie, B.O., Mostafa, M.M.H., Okorator, C. 2021. Durability Assessment and Microstructure of High-Strength Performance Bricks Produced from PET Waste and Foundry Sand. *Materials*, 14, 5635. <https://doi.org/10.3390/ma14195635>  
Aneke, F. I., Mostafa, M. H., and Moubarak, A. 2021. Resilient modulus and microstructure of unsaturated expansive subgrade stabilized with activated fly ash, *International Journal of Geotechnical Engineering*, 15, 915–938, 10.1080/19386362.2019.1656919  
Arati, S., Nagesh, H., Shashishankar, A. 2021. Experimental Studies on Fly Ash Based Lime Bricks, ISSN (Online): 4, 2347–2812.  
ASTM C20-00, Standard Test Methods for Apparent Porosity, Water Absorption, Apparent Specific Gravity, and Bulk Density of Burned Refractory Brick and Shapes by Boiling Water, ASTM International, West Conshohocken, PA, 2000, [www.astm.org](http://www.astm.org)  
ASTM C67, Standard Test Methods for Sampling and Testing Brick and Structural Clay Tile, ASTM International, West Conshohocken, PA, 2003, [www.astm.org](http://www.astm.org)  
ASTM C597-16, Standard Test Method for Pulse Velocity through Concrete, ASTM International, West Conshohocken, PA, 2016, [www.astm.org](http://www.astm.org)  
ASTM D1140. Standard Test Methods for Determining the Amount of Material Finer than 75- $\mu$ m (No. 200) Sieve in Soils by Washing, ASTM International, West Conshohocken, PA, 2017, [www.astm.org](http://www.astm.org)  
ASTM C1012 / C1012M-18b, Standard Test Method for Length Change of Hydraulic-Cement Mortars Exposed to a Sulfate Solution, ASTM International, West Conshohocken, PA, 2018, [www.astm.org](http://www.astm.org)  
ASTM C618-19, Standard Specification for Coal Fly Ash and Raw or Calcined Natural Pozzolan for Use in Concrete, ASTM International, West Conshohocken, PA, 2019, [www.astm.org](http://www.astm.org)

- ASTM C67 / C67M-20, Standard Test Methods for Sampling and Testing Brick and Structural Clay Tile, ASTM International, West Conshohocken, PA, 2020, [www.astm.org](http://www.astm.org)
- ASTM C583-15, Standard Test Method for Modulus of Rupture of Refractory Materials at Elevated Temperatures, ASTM International, West Conshohocken, PA, 2021, [www.astm.org](http://www.astm.org)
- Balksten, K., Strandberg-de Bruijn, P. 2021. Understanding Deterioration due to Salt and Ice Crystallization in Scandinavian Massive Brick Masonry. *Heritage*, 4, 349
- ASTM C597-16, Standard Test Method for Pulse Velocity through Concrete, ASTM 370. <https://doi.org/10.3390/heritage4010022>
- Basha, S.H, Kaushik, H.B. 2014. Evaluation of nonlinear material properties of fly ash brick masonry under compression and shear. *J. Mater. Civ. Eng. (ASCE)* 27, 04014227.
- Council for Scientific and Industrial Research (CSIR). 2014. Economic value of South Africa's waste (preliminary). A waste research, development, and innovation (RDI) roadmap for South Africa. 1, 11–12.
- EPA, Advancing Sustainable Materials Management:2017 Fact Sheet, 2019.
- Eskom, 2015. Eskom Integrated Report IR2015. [www.eskom.co.za/IR2015](http://www.eskom.co.za/IR2015), accessed October 2016.
- Eskom, 2016. Eskom Holdings Ash Strategy 2016–2020. Revision 7. Unpublished data.
- Fei, W., Huiyuan, B., Jun, Y., Yonghao, Z. Correlation of Dynamic and Static Elastic Parameters of Rock, *Electronic Journal of Geotechnical Engineering* 21 1551–1560
- FEVE, Record collection of glass containers for recycling hits 76% in the EU. <https://feve.org/record-collection-of-glass-containers-for-recycling-hits-76-in-the-eu/>, 2019
- Franzoni, E., Gentilini, C., Graziani, G., Bandini, S. 2015. Compressive behaviour of brick masonry triplets in wet and dry conditions. *Constr Build Mater* 82, 45–52. (<https://doi.org/10.1016/j.conbuildmat.2015.02.052>)
- Eliche-Quesada, D., Sánchez-Martínez, J., Felipe-Sesé, M.A. 2019. Silica–Calcareous Non-Fired Bricks Made of Biomass Ash and Dust Filter from Gases Purification. *Waste Biomass Valor* 10, 417–431. (<https://doi.org/10.1007/s12649-017-0056-1>)
- Granneman, S.J., Lubelli, B., Van Hees, R.P. 2019. Mitigating salt damage in building materials by the use of crystallization modifiers—a review and outlook. *J. Cult. Herit.* 2019, 40, 183–194. [CrossRef]
- Hasan, M.R., Siddika, A., Akanda, M.P.A. 2021. Effects of waste glass addition on the physical and mechanical properties of brick. *Innov. Infrastruct. Solut.* 6, 36. <https://doi.org/10.1007/s41062-020-00401-z>
- Kaza, S., Yao, L., Bhada-Tata, P., Van- Woerden, F. 2018. What A Waste 2.0: A Global Snapshot of Solid Waste Management to 2050 (Urban Development Series) (Washington, DC: World Bank) <https://doi.org/10.1596/978-1-4648-1329-0>
- Laven, S., Vosloo, M., Meyer-Douglas, S. 2016. Motivation for the Application for Exemption of Waste Management Activity Licences for Specific Uses of Pulverized Coal Fired Boiler Ash in Terms of GN R. 634. Zitholele Consulting Report 16005-41-Rep-001-Eskom Ash GN, R 634 Application-Rev2
- Liu, Y., Siang, B., Hu, Z., Yang, E. 2017. Autoclaved aerated concrete incorporating waste aluminium dust as a foaming agent, *Constr. Build. Mater.*, 148, 140–147.
- McCormac, J.C., Brown, R.H. 2015. Design of Reinforced Concrete, Wiley, Hoboken, 2015
- Naik, N., Bahadure, B., Jejurkar, C. 2014. Strength and durability of Fly ash, cement and gypsum bricks, *Int. J. Comput. Eng. Res.* 4, 1–4.
- Prabhat, K.S., Rohit, K., Satya, P.D., 2019. Study of Compressive Strength of Fly-SH Brick, *International Journal of Engineering Research & Technology (IJERT)*, 08.
- Pravez, A., Davinder, S., Sanjeev, K. 2021. Incinerated municipal solid waste bottom ash bricks: A sustainable and cost-efficient building material, *Materials Today: Proceedings*, 2021, ISSN 2214-7853, <https://doi.org/10.1016/j.matpr.2021.07.346>
- SANS 227:2007 and SANS 1 575. 2007. the South African National Standard for burnt clay paving units, ISBN 978-0-626-19745-2
- Safeer, A., Muhammad, A. S., Syed, M.S. K., Muhammad, J.M. 2017. Production of sustainable clay bricks using waste fly ash: Mechanical and durability properties, *Journal of Building Engineering*, 14, 7–14, ISSN 2352-7102, <https://doi.org/10.1016/j.jobe.2017.09.008>.
- Sarkar, N., Faris, A. 2019. Mechanical properties of clay masonry units: Destructive and ultrasonic testing, *Construction and Building Materials*, 219, 2019, 111–120, ISSN 0950-0618, <https://doi.org/10.1016/j.conbuildmat.2019.05.166>
- Shaqour, E.N., Abo Alela, A.H. and Rsheed, A.A. 2021. Improved fired clay brick compressive strength by recycling wastes of blacksmiths' workshops. *J. Eng. Appl. Sci.* 68, 5. <https://doi.org/10.1186/s44147-021-00002-2>
- Stefanidou, M., Papayianni, I., Pachta, V. 2015. Analysis and characterization of Roman and Byzantine fired bricks from Greece. *Mater Struct* 48, 2251–2260. <https://doi.org/10.1617/s11527-014-0306-7>
- Sufian, M., Ullah, S., Ostrowski, K.A., Ahmad, A., Zia, A., Śliwa-Wieczorek, K.; Siddiq, M.; Awan, A.A. 2021. An Experimental and Empirical Study on the Use of Waste Marble Powder in Construction Material. *Materials*, 14, 3829. <https://doi.org/10.3390/ma14143829>
- Sutas, J., Mana, E., Arpapan, S., Watcharakhon, N. 2018. Effect of bagasse and bagasse ash levels on properties of pottery products, *Heliyon*, 4, e00814, ISSN 2405-8440, <https://doi.org/10.1016/j.heliyon.2018.e00814>
- Syed, M.S.K., Safeer, A., Muhammad, A. S, Muhammad, J. M., Anwar, K. 2016. Manufacturing of sustainable clay bricks: Utilization of waste sugarcane bagasse and rice

- husk ashes, *Construction and Building Materials*, 120, 29–41, ISSN 0950-0618, <https://doi.org/10.1016/j.conbuildmat.2016.05.084>
- Ukwatta, A., Mohajerani, A., Eshtiaghi, N., Setunge, S. 2016. Variation in physical and mechanical properties of fired-clay bricks incorporating ETP biosolids, *J. Clean. Prod.* 10.1016/j.jclepro.2016.01.094
- Velasco, P., Ortiz, M., Giro, M., Velasco. L. 2014. Fired clay bricks manufactured by adding wastes as sustainable construction material – a review, *Constr. Build. Mater.* 63 (2014) 97–107.
- Yehia S, El-Didamony, and M., Elsayed, T. 2017. Low-cost housing in Egypt by using stabilized soil bricks. *International Journal of Civil, Mechanical and Energy Science* 3, 154–165 <https://doi.org/10.24001/ijcmes.3.3.1>
- Yongue-Fouateu. R, Ndimukong, F., Njoya, A., Kunyukubundo, F., Mbih, P.K. 2016. The Ndop plain clayey materials (Bamenda area-NW Cameroon): Mineralogical, geochemical, physical characteristics and properties of their fired products, *J. Asian Ceram. Soc.* 4, 299–308. 10.1016/j.jascer.2016.05.008
- Yu, J.-H., Park, J.-H. Compressive and Diagonal Tension Strengths of Masonry Prisms Strengthened with Amorphous Steel Fiber-Reinforced Mortar Overlay. *Appl. Sci.* 2021, 11, 5974. <https://doi.org/10.3390/app11135974>